Recent radial growth decline in response to increased drought conditions in the northernmost *Nothofagus* populations from South America

Alejandro Venegas-González[a,*], Fidel Roig Juñent[b], Alvaro G. Gutiérrez[c], Mario Tomazello Filho[a]

[a] *Departmento de Ciências Florestais, Universidade de São Paulo, Avenida Pádua Dias 11, 13418-57 2 Piracicaba, Brazil*
[b] *Laboratorio de Dendrocronología e Historia Ambiental, IANIGLA, CCT CONICET Mendoza, CC 330, M5502IRA Mendoza, Argentina*
[c] *Departamento de Ciencias Ambientales y Recursos Naturales Renovables, Facultad de Ciencias Agronómicas, Universidad de Chile, Santiago, Chile*

ARTICLE INFO

ABSTRACT

An emerging phenomenon of forest decline in Mediterranean-type ecosystems has been detected in response to climate change during the last century. It is expected that the Mediterranean regions will likely experience drought events during this century with consequences for biodiversity maintenance. Although the Chilean Mediterranean-type forests are among the most threatened forest ecosystems in South America, their responses to recent increased drought events due to global warming are poorly documented. In the same region, the endangered and endemic forests of *Nothofagus macrocarpa* (Nothofagaceae) are found on mountain peaks. It is unclear how *N. macrocarpa* forests are responding to increased drought conditions occurring in the area over the last few decades. Here, we analyzed how recent climatic variability has affected the growth of *N. macrocarpa*. We selected five sites along the whole geographic distribution of *N. macrocarpa* forests in central Chile (32.5–34.5°S) to develop tree-ring chronologies. Climate-growth relationships were analyzed through correlations with local (precipitation, temperature and drought index) and large-scale climate data (ENSO index and Antarctic Oscillation). *N. macrocarpa* growth was positively influenced by May to November precipitation (austral winter-spring seasons) and negatively influenced by temperature from October to December (austral spring/early-summer seasons). Using a piecewise regression analysis, we identified a significant decrease in growth from 1980 onwards that resembled a precipitation decline and temperature increase in central Chile during the same time period. Tree-ring chronologies were positively correlated to the ENSO index and negatively correlated to the Antarctic Oscillation index during the current growing season, and more strongly from 1980 onwards. Based on our results, we conclude that increased drought conditions have produced a decline in radial growth of *N. macrocarpa* forests in the last decades. We propose that increased drought conditions predicted for this century in this region will exacerbate this declining *N. macrocarpa* growth trend with unknown consequences for the survival of these endemic and endangered forest ecosystems.

1. Introduction

Mediterranean-type forests are generally characterized by dry summers, and represent biodiversity hotspots because they are found in the most populated areas of the world, and maintain high and endemic species richness (Myers et al., 2000). It is expected that the Mediterranean region will likely experience the greatest proportional change in biodiversity on terrestrial ecosystems because of the substantial influence of different drivers, mainly climate change (Sala et al., 2000). An emerging global pattern of tree mortality has been detected in different Mediterranean forests in response to droughts during the last century (Allen et al., 2010). For example, droughts in the

Mediterranean Basin have intensified at the end of the 20th century compared to their natural variability over the last 900 years (Cook et al., 2016; Gea-Izquierdo and Cañellas, 2014; Sarris et al., 2011). In Mediterranean ecosystems of central Chile, the severity of recent drought events has been cataloged as unprecedented climatic events for the last century in the context of the previous six centuries (Christie et al., 2011). Therefore, a better understanding of Mediterranean forests responses to increased drought conditions is increasingly needed.

The Mediterranean forests of central Chile (MFCC) are within the most threatened ecosystems in South America (32°-35°S; Myers et al., 2000; Schulz et al., 2010; Hernández et al., 2016). The MFCC provide multiple ecosystem services for the most populated area of Chile, and

play an important role in adaptation and mitigation of climate change effects (Donoso and Otero, 2005; Schiappacasse et al., 2012). However, the geographical distribution of MFCC has considerably diminished at a rate of 1.7% per year since 1975 due to urban pressure, commercial forest and crop plantations, wildfire, and unsustainable logging (Donoso, 1982; Miranda et al., 2016; Schulz et al., 2010).

Some of the most vulnerable Mediterranean forests of central Chile are those dominated by *Nothofagus macrocarpa* (DC.) Vásquez and Rodr (Nothofagaceae). This tree species is endemic to central Chile, represents the northernmost distribution of *Nothofagus* in America (Amigo and Rodriguez-Guitian, 2011), and conforms a remnant of relict forests from the last glacial period (Villagrán, 1995). The *N. macrocarpa* forests are fragmented in isolated populations found on the mountain peaks of central Chile (Gajardo, 2001). *N. macrocarpa* form distinct and annual growth rings (Donoso et al., 2010) making it feasible to study its growth sensitivity to climatic variability. The distribution of *N. macrocarpa* covers approximately the latitudinal distribution of MFCC (Amigo and Rodriguez-Guitian, 2011), allowing for the understanding of regional climatic factors that may affect tree growth along the MFCC geographical distribution. The same region is currently affected by drought conditions lasting > 5 years and unprecedented heat during summer (i.e. −21% rainfall, leading to marked decline in water reservoirs and an extended forest fire season; Boisier et al., 2016). These increased drought conditions (i.e. precipitation decrease and temperature increase) are an unprecedented climatic trend from 1850 (Le Quesne et al., 2009).

The inter-annual climate variability in central Chile is influenced by two outstanding modes of global climatic variability, as represented by El Niño-Southern Oscillation (ENSO) and the Antarctic Oscillation (AAO) (Christie et al., 2011). ENSO is a phenomenon characterized by unusual change of the sea surface temperature (SST) in the equatorial central/eastern Pacific Ocean that is warmed (cooled) during El Niño (La Niña) events (Trenberth, 1997). AAO (also referred as the Southern Annular Mode) is a non-seasonal atmospheric circulation variation that occurs south of the 20°S, and is characterized by pressure anomalies of one sign centered in the Antarctic and anomalies of the opposite sign on a circumglobal band at about 40–50°S (Thompson and Wallace, 2000). Both atmospheric circulation patterns have a strong influence on precipitation and temperature in central Chile (Montecinos and Aceituno, 2003; Garreaud et al., 2009), and are indirectly affecting tree growth because of their effect on local climate variability (e.g. Álvarez et al., 2015; Villalba et al., 2012).

In this study, we analyzed the interaction between climate variability and radial growth along the whole distribution of *N. macrocarpa* in South America for the last 150 years. To the best of our knowledge, the growth response of the endemic *N. macrocarpa* forests to recent climatic trends has not been documented. Such an evaluation is critical to understand the dynamics of these Mediterranean forest ecosystems in response to climate change (Gazol et al., 2017). Specifically, we assessed (i) which climate variables best explain the radial growth variability of *N. macrocarpa* at different spatial and temporal scales, (ii) how global climatic oscillations (AAO and ENSO) affect radial growth? and (iii) whether there is a distinguishable growth trend of *N. macrocarpa* in response to recent climate change in central Chile.

2. Material and methods

2.1. Study sites

We selected five sites along the remnant geographic distribution of *N. macrocarpa* forests from Mediterranean-type forests of central Chile (MFCC) (32°57-34°52′S, Fig. 1a, Table 1). In this region shrubland and thorns steppes cover most of the lower hillslopes and piedmont, while creeks and mountain tops are dominated by open forests of evergreen and sclerophyllous tree species. *N. macrocarpa* forests are located at the highest elevations of mountains (between 1000–1800 m a.s.l.) and

represent isolated populations throughout its distribution area (Fig. 1b, Donoso, 1982; Gajardo, 2001). The *N. macrocarpa* patches are scattered in the most industrial and densely human populated area of the MFCC, from where wood has historically been exploited (Gajardo, 2001; Schulz et al., 2010). Therefore, forest patches are mainly young secondary forests with the exception of the old-growth *N. macrocarpa* forests at Alto Huemul and Alto Cantillana sites. There are no studies of cambial activity in this species, but it is expected that the growing season occurs from September to March as suggested by the presence of green foliage during the year (observations *in situ*).

The climate where the MFCC are distributed is Mediterranean, with a dry period of 5–7 months and a total annual precipitation between 300 and 600 mm, and a mean annual temperature between 11 and 13.5 °C modified by latitude and elevation (see also Supporting Information, Fig. S1; Luebert and Pliscoff, 2006). The total annual precipitation has a year-to-year variation in response to climatic oscillation such as El Niño Southern Oscillation (ENSO) and the Antartic Oscillation (AOO) (Garreaud et al. 2009). Forest in the Andes Mountain develop on soils originated from volcanic or granitic rocks and from glacial sediments (Villagrán, 1995). Along the Coastal range, soils are formed from granitic rocks and are poorly developed, usually from residuals on rocky outcrops (Donoso, 1982).

2.2. Tree sampling and ring-width chronologies

At each site, we sampled two or three populations, with the exception of Robleria del Cobre de Loncha where one population was sampled (Table 1). All populations were sampled in April-May 2015, so the last ring formed is from 2014 according to Schulmann's convention for the Southern Hemisphere (i.e. biological year does not coincide with calendar year, (Schulmann, 1956). At each population, we cored around 15 trees in an area of 0.5–1 ha of forest. We randomly selected trees in order to sample different stem sizes, thus avoiding bias in the selection of individuals, and including young and adult trees (Nehrbass-Ahles et al., 2014). We obtained two to three cores per tree at 1.3 m stem height using increment borers. We processed cores using standard dendrochronological methods (Stokes and Smiley, 1996). We examined cores under a stereomicroscope (×10 magnification) and identified the boundary of each tree ring. *N. macrocarpa* has diffuse-porous wood, thus we recognized tree-ring boundaries by the presence of a thin layer of thick-walled fibers at the latewood (Fig. 1c). We measured tree-ring widths using a scanned image of each core at 2400-dpi resolution with a reference scale (ImageJ software, Rasband, 1997).

We used the software COFECHA to statistically validate the cross-dating and measurement quality of each core, and to find potential errors during the dating stage (Holmes et al., 1986). We constructed a chronology for each site by pooling all tree ring series of their populations, using the ARSTAN software. ARSTAN removes the biological age trend of individual tree series and any other stand-dynamics trends (Cook, 1985). For this procedure, we used a cubic spline with a 50% frequency response cutoff equal to 67% of the series length, thus isolating the high frequency variability. We used the residual chronology for the analyses in order to remove its temporal autocorrelation (Cook et al., 1990).

We characterized site chronologies using ring widths average and standard deviation, mean sensitivity (MS), series intercorrelation (SI), Running Bar (RBar), first-order autocorrelation (AR1) and expressed population signal (EPS) (Fritts, 1976). MS represents the mean percentage change of year-to-year growth variability. SI is the mean value of all possible correlations between individual series. RBar describes the mean correlation coefficient for all possible pairings of ring-width series over a common time. AR1 is a measure of the association between tree-ring growths in two consecutive years (Holmes et al., 1986). EPS measures the strength of the common signal in a chronology over time and verifies the hypothetically perfect chronology, with a theoretical threshold ≥ 0.85 (Wigley et al., 1984). MS, SI and AR1 were calculated
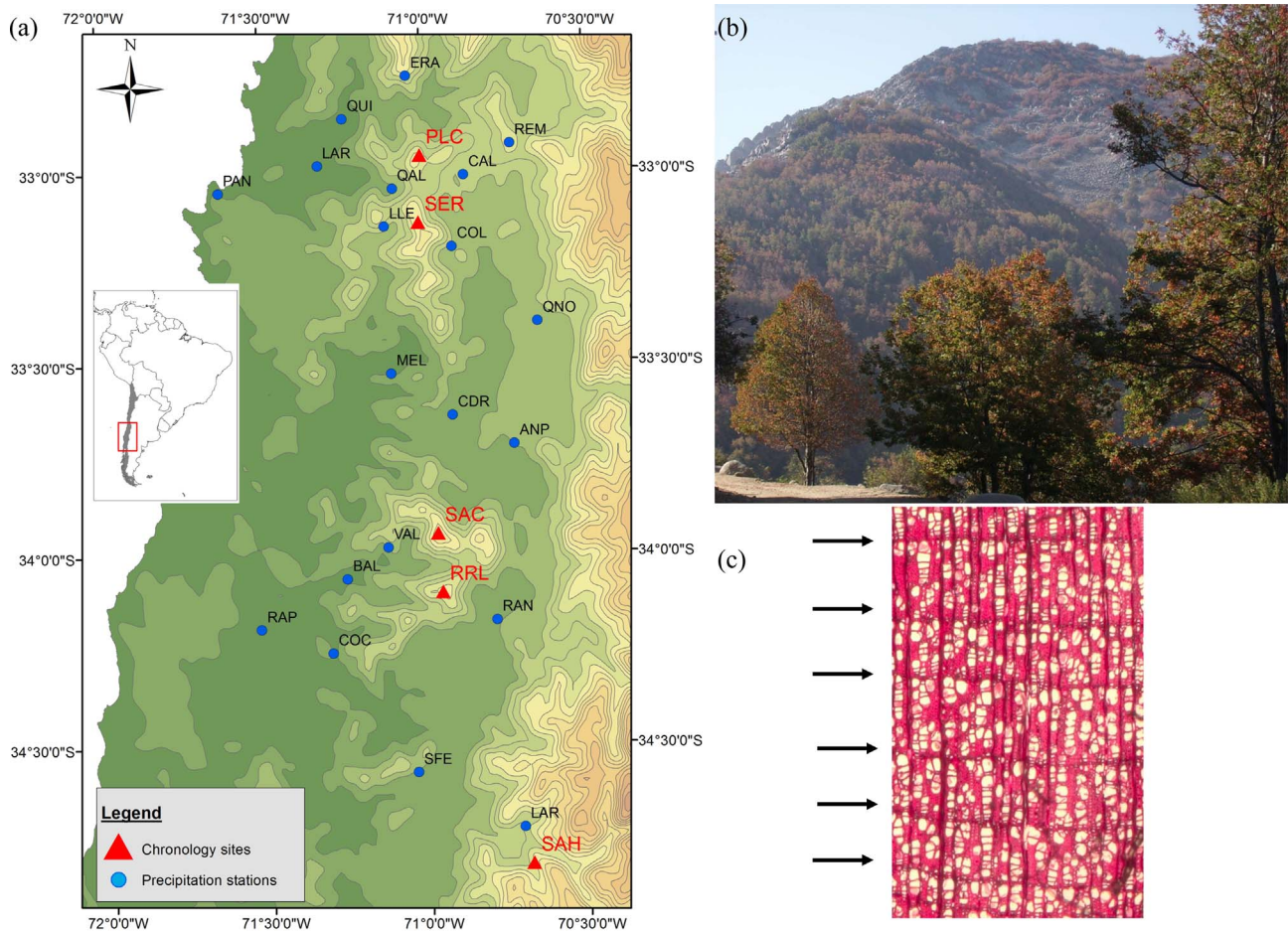
Fig. 1. (a) Study sites (red triangles) and precipitation stations (blue circles) in central Chile (see Table 1 for site acronyms). Contour lines show the shape of the terrain, with elevation lines every 250 m a.s.l. (dark green showing the lowest elevation) and (b) *N. macrocarpa* forest at El Roble site when autumn is starting. (c) Anatomical structure of annual tree rings of *N. macrocarpa*.

on tree-ring width series, while RBAR and EPS are based on residual series.

Regional chronology was calculated as the robust biweighted mean of all available tree ring indices in a given year. Also, we used a principal component analysis (PCA) to identify the common growth pattern variability among the site chronologies. The first principal component (PC1) is commonly used to analyze the tree-ring sensitivity to climate based on mean residual series, which estimates the common variability in growth among all sites, explaining the larger percentage of the climate-related variance (e.g. Lara et al., 2005). Piecewise regression models of tree-ring width were used to analyze the significant change in temporal trends using years as the independent variable. To this end, we used the *segmented* package in R (Muggeo, 2008; R core Team, 2017). This analysis detects the most significant break years between two consecutive segments of variable length in the time series, which corresponds to the year showing the minimum mean squared error.

2.3. Climatic data

To analyze the effect of local climate variability on tree growth, we used monthly climatic data of total precipitation and mean temperature. We obtained instrumental weather records from 20 meteorological stations closest to our study sites (http://explorador.cr2.cl/) (Table 1, Fig. 1a). For precipitation, we used a composite record resulting from the average of two to six stations nearest to each site chronology in the common period 1943–2014 (Table 1). For temperature, we used gridded datasets of reconstructed temperature from CRU TS3.24 produced by the Climate Research Unit (Royal Netherlands Meteorological

Institute, https://climexp.knmi.nl/), with 0.5° spatial resolution for the period 1901–2014 (Table 1). To analyze the climate–growth relationship at a regional level, we estimated regional climatic anomalies (period 1930–2014) by averaging the standard deviations from monthly precipitation or monthly mean temperature using the software MET from the DPL program (Holmes, 1992).

To study the relationship between hydric balance and tree growth, we used the drought index Standardized Precipitation–Evapotranspiration Index (SPEI, 0.5° spatial resolution for the period 1901–2014), which is based on a combination of precipitation and temperature from the same spatial dataset of CRU (Vicente-Serrano et al., 2010). SPEI data was extracted from the KNMI Climate Explorer (https://climexp.knmi.nl/). This index has the advantage of combining a multiscalar character for drought assessment through a basic water balance calculation. Additionally SPEI implies a memory effect on the evapotranspiration rate. SPEI has been widely used in recent dendrochronological studies to understand drought-growth relationship (Camarero et al., 2013; Labuhn et al., 2016).

To analyze the large-scale climate variability on tree growth, we analyzed two global atmospheric circulation indexes, El Niño/Southern Oscillation (ENSO) and Antarctic Oscillation (AAO). ENSO was analyzed by the Multivariate ENSO Index (MEI) for the time period of 1950–2014 (obtained from http://www.esrl.noaa.gov/psd/enso/mei/table.html). This index is based on six main variables observed over the tropical Pacific: sea level pressure, zonal and meridional components of the surface wind, sea surface temperature, air temperature, and total cloudiness fraction of the sky (Wolter and Timlin, 2011). In the case of the tropospheric circulation south of 20° S, we used the Antarctic

Table 1
Site characteristics of the tree-ring chronologies and meteorological stations used in this study.

Site (Code)	Time period	Latitude (S)	Longitude (W)	Elevation (m a.s.l.)
La Campana (PLC)	1904–2014	32°57.7′	71°07.5′	1280
El Roble (SER)	1845–2014	33°00.5′	71°01.5′	1600
Altos Cantillana (SAC)	1789–2014	33°55.1′	70°58.5′	1800
Robleria del Cobre de Loncha (RRL)	1858–2014	34°07.6′	70°57.9′	1.090
Alto Huemul (SAH)	1767–2014	34°51.9′	70°40.2′	1550
Precipitation data obtained from Centro de Ciencia del Clima y la Resiliencia (CR[2] Explorador Climatico)				
Estero Rabuco[1] (ERA)	1965–2014	32°50.8′	71°07.4′	300
Quillota[1] (QUI)	1978–2014	32°53.7′	71°12.5′	130
Los Aromos[1] (LAR)	1974–2014	32°57.4′	71°20.7′	100
Punta Angeles[1] (PAN)	1899–2014	33°01.0′	71°38.0′	41
Caleu[1,2] (CAL)	1957–2014	33°00.3′	70°59.6′	1120
Rungue Embalse[1,2] (REM)	1943–2014	33°01.1′	70°54.5′	700
Quebrada Alvarado[2] (QAL)	1990–2014	33°03.0′	71°06.0′	290
Colliguay[2] (COL)	1950–2014	33°10.1′	71°08.8′	490
Lliu-Lliu Embalse[2] (LLE)	1978–2014	33°05.9′	71°12.8′	260
Quinta Normal[2,3] (QNO)	1899–2014	33°26.7′	70°40.9′	527
Melipilla[3] (MEL)	1971–2014	33°40.8′	71°11.9′	168
Angostura de Paine[3] (ANP)	1988–2014	33°48.2′	70°52.6′	350
Carmen de las Rosas[3,4] (CDR)	1931–2014	33°45.5′	71°09.0′	165
Villa Alhue[3,4] (VAL)	1979–2014	34°02.1′	71°05.6′	197
Rapel[3,4] (RAP)	1940–2014	34°56.7′	71°05.1′	16
Barrera Loncha[4] (BAL)	1984–2014	34°04.9′	71°11.3′	144
Rancagua[4] (RAN)	1910–2014	34°11.4′	70°45.0′	515
Cocalan[4] (COC)	1978–2014	34°12.1′	71°16.5′	120
San Fernando[5] (LAR)	1910–2014	34°35.1′	71°00.0′	350
La Rufina[5]	1930–2014	34°44.5′	70°45.1′	743
Temperature data from Royal Netherlands Meteorological Institute (KNMI Climate Explorer)				
CRU TS3.24[1]	1901–2014	32°30′/33°00′	71°30′/71°00′	–
CRU TS3.24[2]	1901–2014	33°00′/33°30′	71°00′/70°30′	–
CRU TS3.24[3]	1901–2014	33°30′/34°00′	71°00′/70°30′	–
CRU TS3.24[4]	1901–2014	34°00′/34°30′	71°00′/70°30′	–
CRU TS3.24[5]	1901–2014	34°30′/35°00′	71°00′/70°30′	–

Numbers indicate sites where the meteorological station were used for analysis.

[1] PLC,
[2] SER,
[3] SAC,
[4] RRL,
[5] SAH.

Oscillation index (AAO) for the time period 1948–2011 (obtained from http://jisao.washington.edu/data/aao/slp/). This index is based on principal components of geodynamic height anomalies at 850 hPa (Thompson and Wallace, 2000) and represents the variability in the extratropical atmospheric circulation, accounting for ca. 1/3 climate variability of the Southern Hemisphere (Marshall, 2003). The AAO positive phase is associated with decreased (increased) sea level surface pressure over Antarctica (mid-latitudes) in the austral summer (Garreaud et al., 2009).

2.4. Statistical analyses

We evaluated the effect of climate variables (precipitation, temperature, SPEI, MEI and AAO) on tree growth (ring-width index for each site and PC1 for regional chronology) using a correlation function analysis, i.e. tree growth was considered as an integration of climate influences occurring from prior to current growing periods (Fritts, 1976). For this analysis, we correlated ring-width against the time period covering from January of the previous year to March of the current year. We analyzed temporal trends in correlation coefficients between regional chronology and climate by bootstrapped moving correlation intervals of 30 years (Biondi, 1997) using the Dendroclim2002 software (Biondi and Waikul, 2004).

We explored the link between drought events in central Chile documented by Le Quesne et al. (2006), Garreaud et al. (2017) and SPEI (1-month) with our ring-width chronology. We classified years by two types of low tree-growth (i.e. negative pointer years) related to drought

using a threshold of ≤1.0 (strong effect) and ≤2.0 (severe effect) standard deviations below the mean of the residual regional chronology.

To analyze spatial correlations at a regional scale, we correlated PC1 against precipitation (CRU TS3.24 land), temperature (CRU TS3.24 land) and SPEI (1-month), using a resolution of 0.5° × 0.5° gridded cells. At a global scale, we correlated PC1 against (i) ENSO using the sea surface temperature (SST) of the equatorial Pacific region (HadISST1 1.0° reconstruction), and (ii) AAO using the sea level pressure (SLP) across the northern Antarctic Ocean (HadLSP2 5.0° reconstruction). We used spatial field correlations from the KNMI (Royal Netherlands Meteorological Institute) using the data available from the Climate Explorer Website (http://climexp.knmi.nl/). Finally, we performed a continuous Wavelet Transform analysis (Torrence and Compo, 1998) for the regional chronology of *N. macrocarpa* to determine the main oscillatory cycles and to localize intermittent periodicities.

3. Results

3.1. Characteristics of tree-ring chronologies

We obtained cores from 146 trees with ages ranging between 22 and 248 years (Table 2). Tree-ring chronologies obtained from northern stands (PLC and SER) covered a shorter time period compared to southern stands (Fig. S2). All five sites had high mean sensitivity and intercorrelation between series (> 0.39 and > 0.47, $P < .01$, respectively). RBar varied between 0.19 (SAH) and 0.27 (PLC). The expressed

Table 2
Descriptive statistics for the five *N. macrocarpa* chronologies developed in this study (see Table 1 for chronology code definitions). Site acronyms as in Table 1.

Variables	Sites					
	PLC	SER	SAC	RRL	SAH	Regional
No. trees (sampled)	30	30	27	24	44	155
No. trees (chronology/radii)	29/47	29/42	24/46	23/37	41/56	146/228
Mean ring width ± SD (mm	1.34 ± 0.88	1.81 ± 1.17	1.39 ± 0.78	1.69 ± 0.90	1.39 ± 0.73	1.49 ± 0.86
Time span (> 5 trees)	1929–2014	1921–2014	1826–2014	1890–2014	1832–2014	1832–2014
Age ± standard deviation	69 ± 17	72 ± 25	140 ± 73	88 ± 55	120 ± 110	98 ± 55
Mean sensitivity	0.45	0.50	0.47	0.4	0.39	0.44
Series intercorrelation	0.60	0.52	0.51	0.49	0.47	0.43
RBar (± SE)	0.27 ± 0.01	0.25 ± 0.02	0.25 ± 0.02	0.21 ± 0.03	0.19 ± 0.02	0.12 ± 0.01
First-order autocorrelation	0.60	0.49	0.47	0.54	0.60	0.54
Period with EPS ≥ 0.85	1930–2014	1945–2014	1885–2014	1910–2014	1860–2014	1905–2014

population signal was ≥0.85 from 1930 (PLC), 1945 (SER), 1885 (SAC), 1910 (RRL) and 1860 (SAH) to 2014, indicating that sampling replication was adequate in those periods (Table 2). The correlation matrix showed that all chronologies somehow correlated among themselves (r > 0.3, P < .01, Fig. S3).

3.2. Regional chronology and trends

We developed a regional chronology of 228 series (146 trees) for the whole distribution of *N. macrocarpa* covering the period 1832–2014 (> 10 trees), with intercorrelation between series of 0.43 and mean sensitivity 0.44, and EPS ≥ 0.85 for the period 1905–2014 (Table 2). The principal component analysis (PCA) of the five residual chronologies for the common period (1929–2014) showed that the first principal component (PC1) contributed to 60.8% of the total variance and the PC2 contributed 15.7% of the variance, with all sites showing positive loadings (see also Fig. S4).
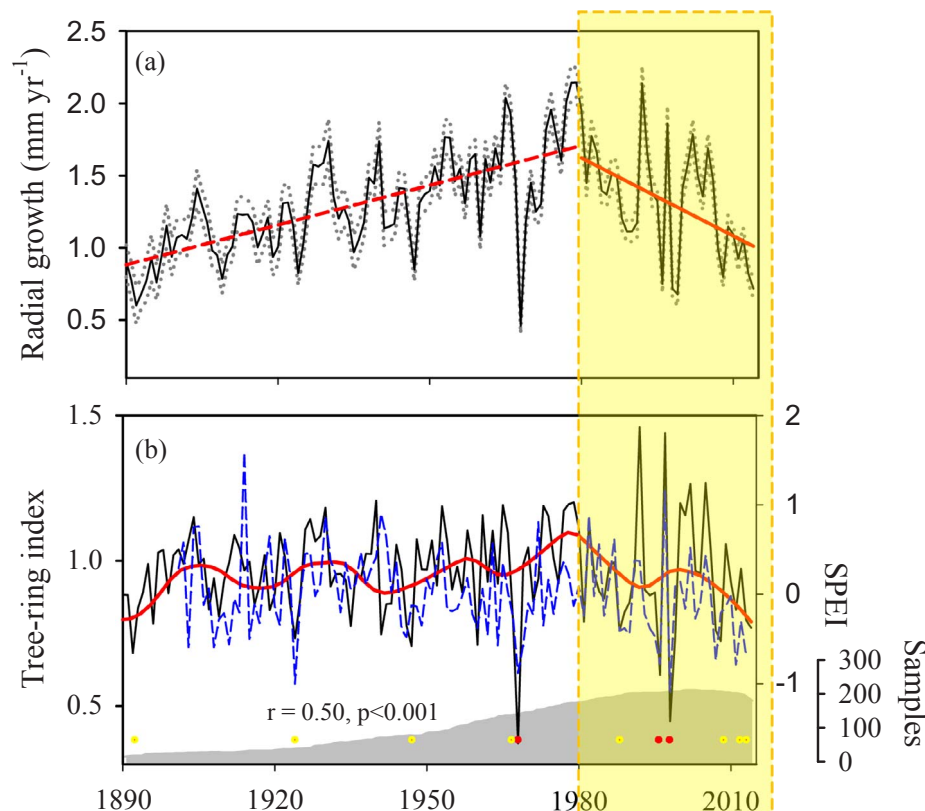
The piecewise regression model identified a significant decrease in the radial growth of *N. macrocarpa* trees after 1980 (Fig. 2a). Regional chronology showed negative pointer years that coincide with drought years identified by Le Quesne et al. (2006) and Garreaud et al. (2017). The drought years reflected in the regional chronology were 1892, 1924, 1946, 1967, 1968, 1988, 1996, 1998, 2007, 2013 and 2014 (Fig. 2b). Three drought years had a severe effect on tree-ring growth (≤2.0 standard deviations below the mean of residual regional chronology) and two of them occurred in the 1990s. We detected an increase of years with low tree growth linked to drought in the residual tree-ring chronology for the 1980–2014 period. These responses represent 55% of 11 years with lowest tree growth related to drought in central Chile.

3.3. Spatio-temporal climate-growth relationships

3.3.1. Local scale

Overall, all tree-ring chronologies correlated with climate (Figs. 3 and 4). We detected significant correlations with monthly precipitation during the late austral autumn to austral spring (from May to November) and an inverse relationship with monthly mean temperature

Fig. 2. (a) Regional chronology of *Nothofagus macrocarpa* (black line, mean radial growth rate (period covered by > 30 trees). Piecewise regression model identified 1980 as a break year (p < .001, orange rectangle). (b) Residual regional chronology of *N. macrocarpa* (black lines) including the five sites for period 1890–2014 (> 30 trees) and SPEI chronology for May to November calculated at one-month scale (dashed blue line) for the period 1901–2014. Circles represent the lowest tree growth that coincides with drought years identified also by Le Quesne et al. (2006) and Garreaud et al. (2017). Yellow and red circles indicate years with ≤1.0 (strong effect) and ≤2.0 (severe effect) standard deviations below the mean of the residual regional chronology. Residual chronology smoothed is shown with a cubic spline (red line) designed to reduce 50% of the variance in a sine wave with a periodicity of 20 years (Cook et al., 1990). The number of samples is indicated by the grey shaded area.
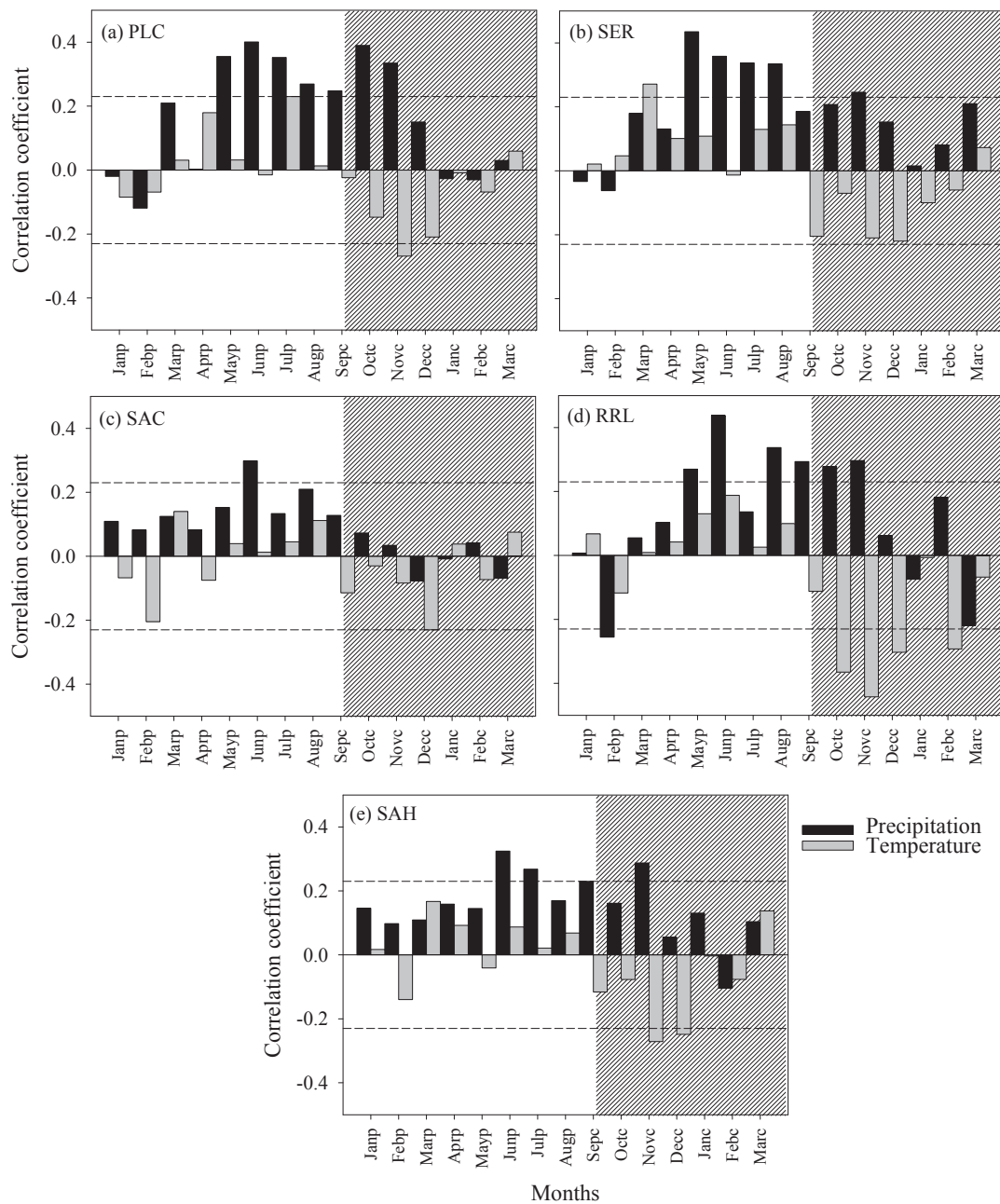
Fig. 3. Correlations between residual chronologies of studied *N. macrocarpa* populations and monthly climatic variables (local scale), during the 1943–2014 (common period). Dashed horizontal lines indicate statistical significance at the 95% confidence level (*r* = ± 0.23). Shaded areas indicate current growing season. Letters beside the months indicate growing periods (p previous year, c current year).

during the austral spring to early austral summer (October to December, Fig. 3). The strongest correlations occurred in June for monthly precipitation (all populations, r ≥ 0.30, *P* < .01, austral winter) and in November (PLC, RRL and SAH, r ≤ −0.27, *P* < .05) and December for monthly temperature (SAC, r ≤ −0.23, *P* < .05) (Fig. 3). Using seasonal means of one-month SPEI, we found a significant correlation of the five *N. macrocarpa* chronologies to wet conditions in winter (r ≥ 0.34, *P* < .01) and spring (r ≥ 0.21, *P* < .10) (Fig. 4a).

3.3.2. Regional

First principal component of the regional tree-ring chronology (PC1) was positively correlated to regional precipitation between May and November (austral winter/austral spring) of the current growing season (*P* < .05, Fig. 5a), for the period 1930–2014, with June precipitation having the highest correlation with PC1 (r = 0.43,

P < .001). PC1 was negatively correlated to regional temperatures of late-spring/early-summer during the current growing season (i.e. October to December, *P* < .05) with November temperature having the highest correlation with PC1 (r = −0.32, *P* < .01, Fig. 5a). The *N. macrocarpa* growth (PC1) was correlated to 1–24-months SPEI (~r = 0.40) for the previous and current growing season (from May to April, Fig. 4b). We found that regional chronology strongly responded to mean one-month SPEI of May to November for the period 1901–2014 (r = 0.50, *P* < .001, Fig. 2b).

Moreover, moving correlations using a 30-year window confirmed that growth response to local and global climate variability has increased since the last three decades of 20th century (Fig. 5c and d). Regarding the local sensitivity, we observed positive correlation with precipitation anomalies (r = 0.71 and *P* < .001, Fig. 6a) and negative correlation with temperature anomalies (r = −0.42 and *P* < .01,
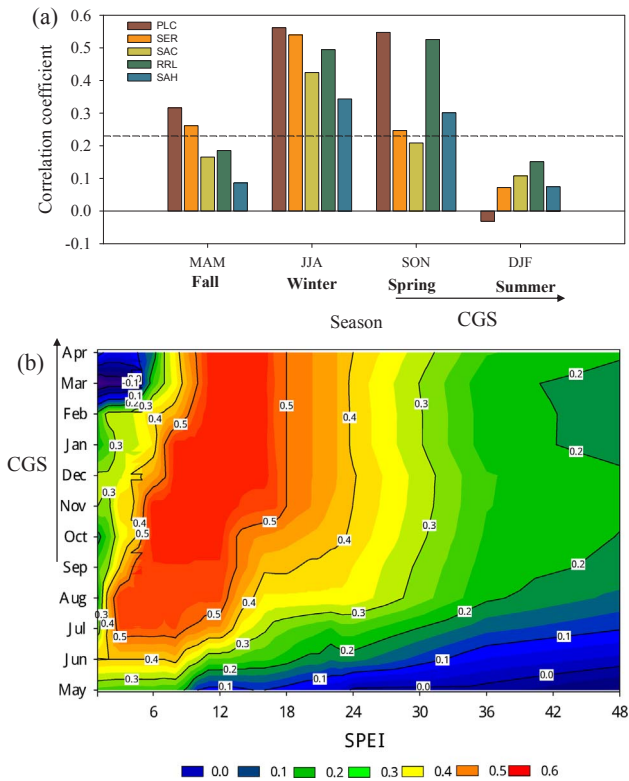
Fig. 4. (a) Correlations between residual chronologies of the five site study of *N. mac-rocarpa* and SPEI drought index (one-month) by season, during 1943–2014 (common period). Dashed horizontal lines indicate statistical significance at the 95% confidence level ($r = 0.23$). (b) Correlations calculated between the first principal component of *N. macrocarpa* sites and SPEI calculated at monthly scales ranging from one to 48 months. Values of the correlation coefficients higher and lower than 0.20 or -0.20 ($P < .05$), respectively. CGS: Current growing season.
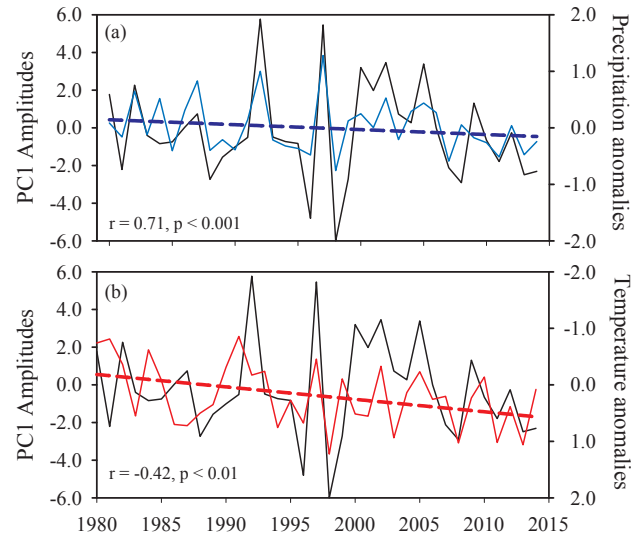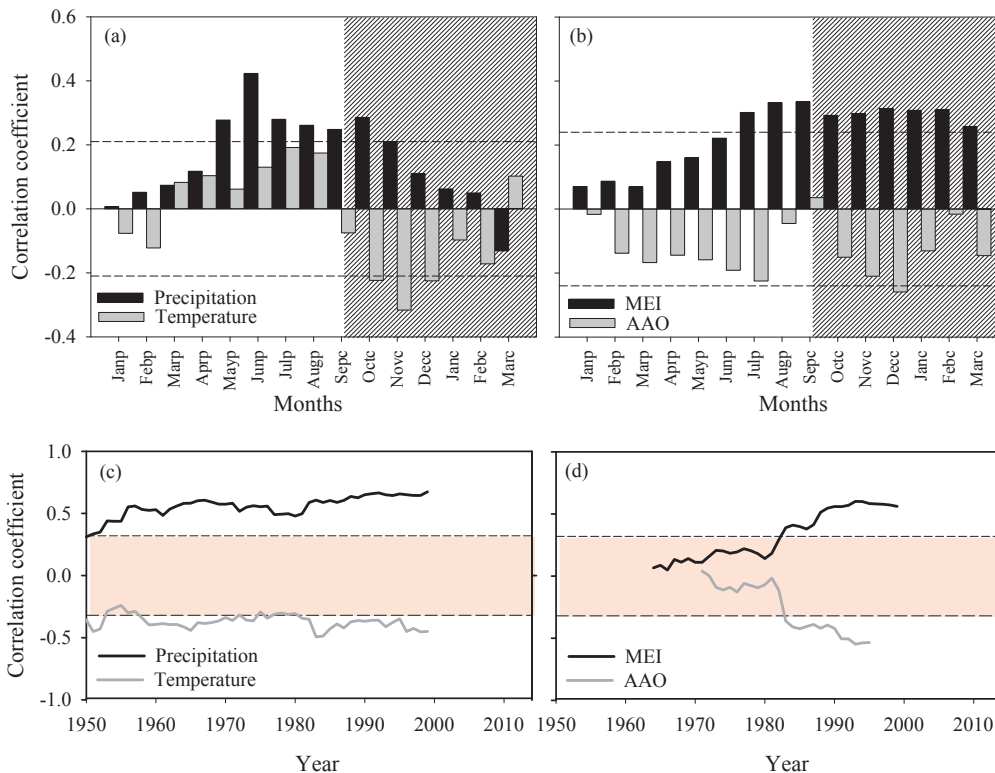

Fig. 6. (a) and (b) Correlations between the first principal component of the tree-ring chronology and anomalies of precipitation (May to November) and temperature (October to December) during the significant months of Fig. 4a, for the period with significant negative decrease trends (1980–2014). Blue and red line indicate the lineal trends ($P < .10$ to precipitation and $P < .01$ to temperature). Note that for temperature, inverse values are used to improve visualization.

Fig. 6b). Spatial correlations verified the high sensitivity of *N. macrocarpa* populations to favorable humidity conditions of austral winter/austral spring in mid-latitudes of South America (30–45°S), for the period 1980–2014 (Fig. 7a).

3.3.3. Global

We found that PC1 was positively correlated to MEI and negatively correlated to AAO (Fig. 5b, $P < .05$). *N. macrocarpa* tree-ring chronology was strongly correlated to MEI, particularly for the period from July to March + 1 (late growing season). In contrast, tree-ring width

Fig. 5. Correlations between the first principal component of the regional chronology of *N. macrocarpa* and: (a) total precipitation and mean temperature during the 1930–2014 common period; (b) Multivariate ENSO index, MEI, period 1950–2014 and Antarctic oscillation, AAO, period 1948–2011. Dashed horizontal lines indicate statistical significance at the 95% confidence level. Shaded areas indicate current growing season. Letters besides the months indicate growing periods (p previous year, c current year). (c) and (d) 30-year moving correlation functions for the significant months of Fig. 4a, b for the period 1950–2014 (precipitation: May to November, temperature: October to December, MEI: July to March + 1, AAO: November to December). It is shown the mid-year of the 30-year interval (i.e. 1950 indicate the interval 1935–1965). Colored areas indicate not significant correlation coefficients.
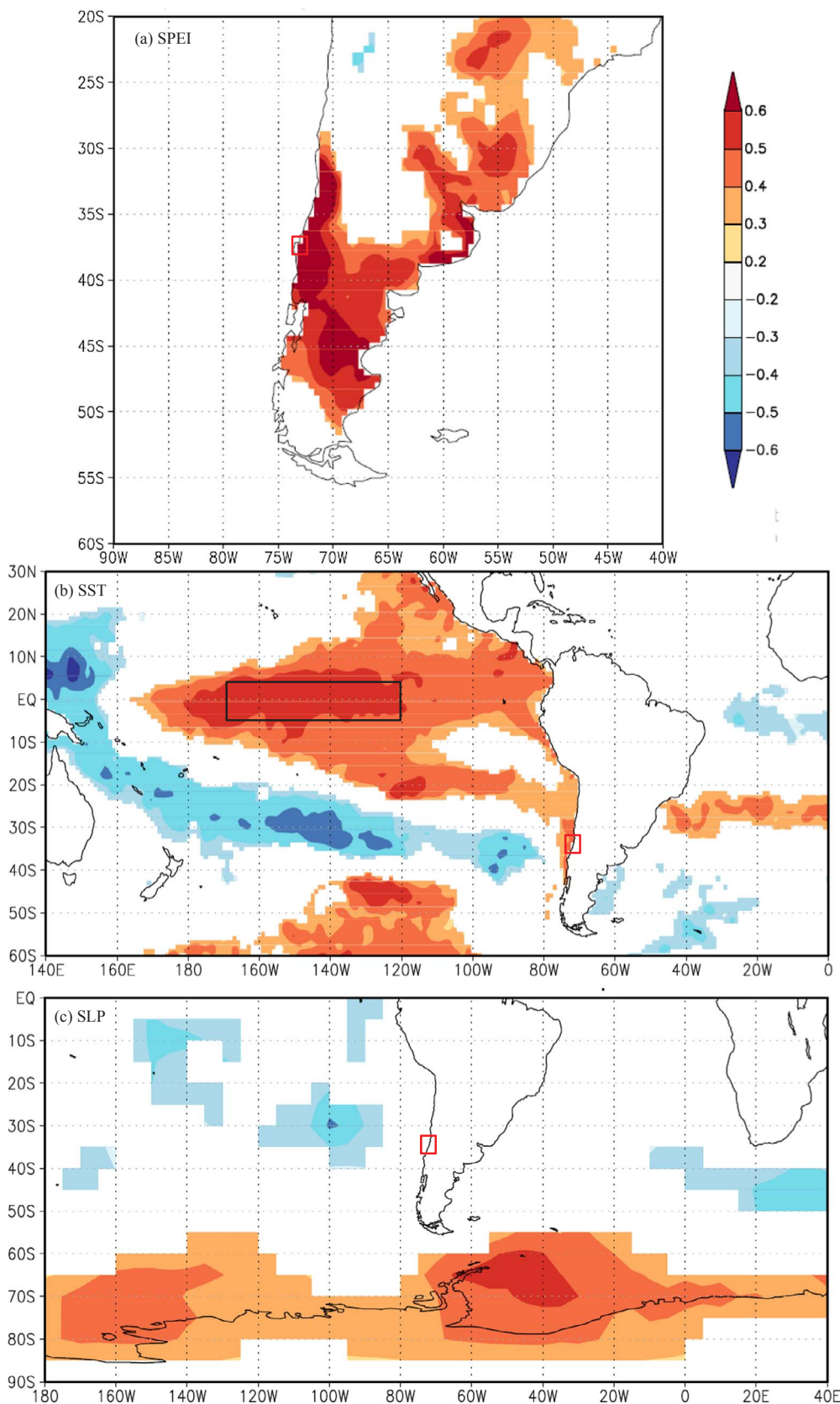
Fig. 7. Spatial correlation fields of regional chronology (PC1) of *N. macrocarpa* and gridded monthly climatic observations for the period 1980–2014 (global scale): (a) Standardized Precipitation-Evapotranspiration Index (SPEI) (calculated at one-months scale) from May to November; (b) Sea surface temperature (SST $1.0° × 1.0°$) from July to March and; (c) Sea level pressure (SLP $5.0° × 5.0°$) of November and December. Colored areas are statistically significant at a 90% level. Study area is indicated by a red square. Niño 3.4 region is indicated by a black rectangle.

was significantly correlated to AAO in December during the current growing season ($r = -0.26$, $P < .05$).

We found the highest spatial correlations with sea surface temperature (SST) and sea level pressure (SLP) after 1980 (Fig. 7b and c).

We also found a significant correlation of tree growth with atmospheric circulations of tropical Pacific and Antarctic regions ($r > 0.50$; $P < .05$). We found a positive association with the sea surface temperature (SST) in the equatorial Pacific, mainly at the Niño 3.4 region
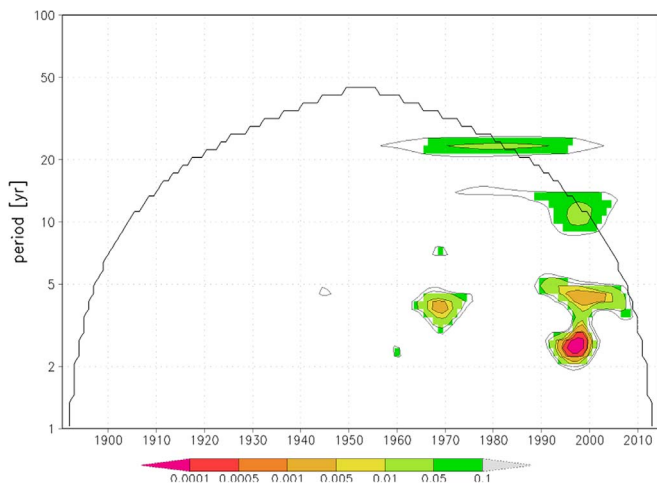
Fig. 8. The wavelet power spectrum of regional chronology. The contour levels were chosen at *P*-value < 0.1. The cross-hatched region is the cone of influence, where zero padding has reduced the variance.

during July and March + 1 (Fig. 7b). Also, we observed a dipole between the SST at the Equator region relative to mid-latitudes (10–40°S), with positive and negative correlations with our regional chronology after 1980. PC1 had a positive correlation with sea level pressure (SLP) throughout the Antarctic region south of 60°S, and negative correlation with SLP at mid-latitudes (Fig. 7c), indicating the inverse association between SLP south of 60°S and AAO.

Spectral analyses for the regional chronology (period 1850–2014) showed significant oscillations at sub-decadal frequencies (< 5 years) mainly during the time periods 1850–1900 and 1970 to present (Fig. 8). We also detected significant oscillations at sub-decadal (i.e. 2.5 and 4.6 years) and multi-decadal frequencies (13.1 and 24.9 years).

4. Discussion

4.1. Impacts of drought on tree-growth chronologies of Nothofagus macrocarpa

Our results demonstrate that radial growth of *Nothofagus macrocarpa* is sensitive to local and regional (to global) climatic variability. We found a decreasing growth trend from 1980 to the present closely following tendencies in winter-spring precipitation (Fig. 6a) and late-spring/early-summer temperatures for the same time period in central Chile (Fig. 6b).

N. macrocarpa populations had comparable responses to climate along its geographic distribution. This was reflected by a large proportion of common inter-annual variations in tree growth (i.e. high percentage of common variance associated with the first principal component) pointing at a regional influence of climate variability on radial growth (Fig. S4). On one hand, winter and early spring rainfall promotes tree growth in *N. macrocarpa* populations (Figs. 3 and 5a) indicating a strong dependence of tree growth on soil water content. On the other hand, warm temperatures constrained tree growth (Fig. 5a). We interpret this result as a negative response of tree growth to drought conditions during the growing season (see also Fig. S1, October to December). Consequently, an increase in temperature during the growing season would promote an increase in evapotranspiration causing a decrease of tree growth in these Mediterranean forests.

In the last three decades, increased drought conditions have become important along the geographic distribution of *N. macrocarpa* compared with previous centuries (Christie et al., 2011; Garreaud et al., 2017; González-Reyes, 2016), a tendency that is significantly expressed in the tree growth reduction detected in our study since 1980 (Figs. 2a, 5c, d, 6a, b). Similar responses of tree growth to climate has

been documented for other tree species along the geographic distribution of Chilean Mediterranean ecosystems, e.g. *Austrocedrus chilensis, Kageneckia angustifolia, Proustia cuneifolia* and *Fabiana imbricata* (Barichivich et al., 2009; Christie et al., 2011; Le Quesne et al., 2006; Urrutia et al., 2011). Also, radial growth reductions of both broadleaved and coniferous trees species have been reported in Mediterranean forests elsewhere, in response to a drier climatic trend since the early 1970–1980s caused by warming without increasing precipitation (e.g. Gea-Izquierdo et al., 2014; Gea-Izquierdo and Cañellas, 2014; Sarris et al., 2011).

The observed climate-growth relationships in *N. macrocarpa* suggest that drought events are the most proximate cause of years with lowest radial growth (negative pointer years) in these forests. Such an effect has also been reported for the coniferous tree species *Austrocedrus chilensis* (Le Quesne et al., 2006), which is mainly found in the Andes mountain in our study region. Interestingly, the severe drought events occurring in 1968, 1996, and 1998 induced strong restrictions to radial growth in these two species. Therefore, we suggest that increased drought conditions are impacting forest growth in both the Coastal and Andes mountains of the Mediterranean region of Chile. Moreover, a significant rainfall decline has been registered in central Chile since 2010 to date, which has decreased water reservoirs and increased the risk of wildfire hazards, among other effects (Garreaud et al., 2017). This last, long-lasting drought event has no precedents in local records and contributes to a drying trend in the region driven by climatic and anthropogenic change (Boisier et al., 2016).

Our results on declining growth rates are in line with findings from other temperate and Mediterranean regions with similar episodes of long-lasting drought during the last few decades. For example, the outstanding extreme heat wave and consequent drought of 2003 produced extensive tree mortality and forest decline of tree species in different parts of Europe (Bréda et al., 2006; Galiano et al., 2010; Rigling et al., 2013; Vennetier et al., 2007). Moreover, several forests across America have experienced extensive disease and mortality coincidently with drought episodes during the 20th-century (Bigler et al., 2007; Negron et al., 2009). On the eastern side of the Andes (Argentina), a negative influence of droughts on forest growth of both broadleaved (*Nothofagus pumilio*) (Lavergne et al., 2015; Rodríguez-Catón et al., 2016) and the conifer *Austrocedrus chilensis* (Mundo et al., 2010) was reported.

In central Chile, global and regional climate models predict a rainfall reduction for the 21st century under a business-as-usual scenario (Quintana and Aceituno, 2012). Based on our results, we propose that predicted increases in drought conditions will exacerbate growth decline in *N. macrocarpa* trees in this century. Such a decreasing growth trend may be intensified in *N. macrocarpa* populations found at the dry edge of its geographic range. However, we expect that along the geographic distribution of *N. macrocarpa*, increased drought conditions will affect the physiology of this species, with trees closing their stomata more frequently to avoid excessive water loss, with a consequent reduction in CO_2 assimilation and biomass production (Granda et al., 2014; Linares and Camarero, 2012). However, tree vulnerability to drought depends on several physiological, genetic and adaptive factors, which are not yet fully understood in current climate change scenarios (Allen et al., 2015; Franklin et al., 1987). The latter is particularly true for *Nothofagus macrocarpa* forests, thus future research addressing mortality caused by ongoing drought conditions in the region is necessary to understand ecological resilience of these forests to ongoing climate change.

4.2. Response of Nothofagus macrocarpa to large-scale climatic variability

Radial growth of *Nothofagus macrocarpa* was sensitive to the inter-annual climate variability in central Chile, which is influenced by two outstanding modes represented by El Niño-Southern Oscillation (ENSO) and the Antarctic Oscillation (AAO) (Garreaud et al., 2009). In central

Chile (30–35°S), above-average precipitation in winter (June to August) coincides with El Niño episodes whereas the opposite occurs during La Niña events (Montecinos and Aceituno, 2003; Quintana, 2000). In our study, we found a positive correlation between the SST anomalies of El Niño 3.4 during the austral winter-spring seasons (July to November) and *N. macrocarpa* tree ring chronology (Figs. 5b and 7b). This result suggests that radial growth increases during El Niño episodes similar to findings from other studies in the Mediterranean-subtropical forests of Chile (Christie et al., 2011; Muñoz et al., 2016). In our study, we found a strong and negative correlation between *N. macrocarpa* tree-ring chronologies and AAO during November–December (austral summer, Fig. 5b). Thompson et al. (2011) suggested a dominance of a positive phase of the Antarctic oscillation (AAO) during summer for the period 1950–2000. This AAO phase may explain the observed downward trend in annual precipitation and temperature increase for central Chile during the same period (Garreaud et al., 2009; Quintana and Aceituno, 2012). Therefore, we suggest that positive phases of AAO during summer would cause a rising temperature in December (warmer early-summer) and reduce precipitation in June (a declining trend of rainiest month), negatively affecting radial growth of *N. macrocarpa*. Accordingly, other studies suggested a similar, indirect influence of AAO on radial growth in temperate and Mediterranean-type forests of South America (Álvarez et al., 2015; Christie et al., 2011; Lara et al., 2015; Villalba et al., 2012).

We observed an increasing correlation strength since 1980 between radial growth of *N. macrocarpa*, MEI and AAO (Fig. 4d) that is consistent with correlations found with SST (Equatorial region) and SLP (Antarctic region, Fig. 7b, c). Furthermore, the spectral analysis of our regional tree-ring chronology showed an oscillatory mode of around 4.3 years (Fig. 8) mimicking the ElNiño 3 SST time series (Torrence and Compo, 1998). This high-frequency domain has also been detected in other tree species of the Mediterranean region of southern South America (Álvarez et al., 2015; Barichivich et al., 2009; Christie et al., 2011; Le Quesne et al., 2009), revealing a non-stationary periodicity at the sub-decadal level. Wavelet power spectrum analysis (Fig. 8) confirmed that the spectral power at interannual time scales is more pronounced for the time period 1990–2010, possibly linked to the 1997–98 ENSO event. Similar teleconnections of atmospheric circulation patterns with tree growth have been found in Mediterranean forest elsewhere. For example, Dorado-Liñan et al. (2017) and Camisón et al. (2016) found a general reduction of tree growth in populations of broadleaved (*Quercus spp*, *Fagus sylvatica* and *Castanea sativa*) and coniferous trees (*Pinus spp*) since 1970–1980s. They linked decreasing growth trends to rising dry and warm conditions during the growing season, which is teleconnected to the strengthening of the Summer North Atlantic Oscillation and to negative phases of the Western Mediterranean Oscillation. Rozas et al. (2015) showed a significant positive association between tree growth of *Fagus sylvatica* over the transitional region of Eurosiberian and Mediterranean forests and ElNiño 3.4 index. Therefore, tree growth of Mediterranean forests in different part of the world seems to respond to global atmospheric circulation patterns. It is predicted that more frequent La Niña events will occur by the year 2100 (Cai et al., 2015) causing frequent and increased drought events in central Chile, potentially increasing the climatic vulnerability of *N. macrocarpa* forests.

5. Conclusions

Here we reported a strong decrease in growth of *Nothofagus macrocarpa*. Our results strongly suggest that radial growth of *N. macrocarpa* is sensitive to local and large-scale (i.e. regional to global) climatic variability, mainly for the period 1980–2014. In these last three decades, we detected a significant decrease in radial growth related to a rainfall decline and temperature increase registered in central Chile (increased drought conditions). Growth tendencies of *N. macrocarpa* were related to changes in high-frequency climatic oscillations (ENSO

and AAO). This result is comparable to responses of Mediterranean forests in the Northern Hemisphere showing significant tree growth declines attributed to drought/heat stress, and thus contribute to the Mediterranean forest biome climate change impact assessment.

According to our results, predicted increases in drought conditions for this century will continue to reduce *Nothofagus macrocarpa* growth and can represent a major threat for the survival of these endemic, relict and endangered forest ecosystems. We based this conclusion on (1) *N. macrocarpa* growth decline following recent changes in the local and global climatic variability, and (2) its restricted geographic distribution found in a region with high human pressure. In order to assess forest persistence, further research is needed on the impact of climate change on mortality, recruitment patterns and genetic variability of these Mediterranean forests.

Appendix A. Supplementary material

Supplementary data associated with this article can be found, in the online version, at http://dx.doi.org/10.1016/j.foreco.2017.11.006.

References

Allen, C.D., Breshears, D.D., McDowell, N.G., 2015. On underestimation of global vulnerability to tree mortality and forest die-off from hotter drought in the Anthropocene. Ecosphere 6, 1–55.

Allen, C.D., Macalady, A.K., Chenchouni, H., Bachelet, D., McDowell, N., Vennetier, M., Kitzberger, T., Rigling, A., Breshears, D.D., Hogg, E.H.T., 2010. A global overview of drought and heat-induced tree mortality reveals emerging climate change risks for forests. For. Ecol. Manage. 259, 660–684.

Álvarez, C., Veblen, T.T., Christie, D.A., González-Reyes, Á., 2015. Relationships between climate variability and radial growth of Nothofagus pumilio near altitudinal treeline in the Andes of northern Patagonia, Chile. For. Ecol. Manage. 342, 112–121.

Amigo, J., Rodriguez-Guitian, M., 2011. Bioclimatic and phytosociological diagnosis of the species of the Nothofagus genus (Nothofagaceae) in South America. Int. J. Geobot. Res. 1, 1–20.

Barichivich, J., Sauchyn, D.J., Lara, A., 2009. Climate signals in high elevation tree-rings from the semiarid Andes of north-central Chile: responses to regional and large-scale variability. Palaeogeogr. Palaeoclimatol. Palaeoecol. 281, 320–333.

Bigler, C., Gavin, D.G., Gunning, C., Veblen, T.T., 2007. Drought induces lagged tree mortality in a subalpine forest in the Rocky Mountains. Oikos 116, 1983–1994.

Biondi, F., 1997. Evolutionary and moving response functions in dendroclimatology. Dendrochronologia 15, 139–150.

Biondi, F., Waikul, K., 2004. DENDROCLIM2002: a C + + program for statistical calibration of climate signals in tree-ring chronologies. Comput. Geosci. 30, 303–311.

Boisier, J.P., Rondanelli, R., Garreaud, R.D., Muñoz, F., 2016. Anthropogenic and natural contributions to the Southeast Pacific precipitation decline and recent megadrought in central Chile. Geophys. Res. Lett. 43, 413–421.

Bréda, N., Huc, R., Granier, A., Dreyer, E., 2006. Temperate forest trees and stands under severe drought: a review of ecophysiological responses, adaptation processes and long-term consequences. Ann. For. Sci. 63, 625–644.

Cai, W., Wang, G., Santoso, A., McPhaden, M.J., Wu, L., Jin, F.-F., Timmermann, A., Collins, M., Vecchi, G., Lengaigne, M., 2015. Increased frequency of extreme La Niña events under greenhouse warming. Nat. Clim. Chang. 5, 132–137.

Camarero, J.J., Manzanedo, R.D., Sanchez-Salguero, R., Navarro-Cerrillo, R.M., 2013. Growth response to climate and drought change along an aridity gradient in the southernmost Pinus nigra relict forests. Ann. For. Sci. 70, 769–780.

Camisón, Á., Silla, F., Camarero, J.J., 2016. Influences of the atmospheric patterns on unstable climate-growth associations of western Mediterranean forests. Dendrochronologia 40, 130–142.

Christie, D.A., Boninsegna, J.A., Cleaveland, M.K., Lara, A., Le Quesne, C., Morales, M.S.,

Mudelsee, M., Stahle, D.W., Villalba, R., 2011. Aridity changes in the Temperate-Mediterranean transition of the Andes since AD 1346 reconstructed from tree-rings. Clim. Dyn. 36, 1505–1521.

Cook, B.I., Anchukaitis, K.J., Touchan, R., Meko, D.M., Cook, E.R., 2016. Spatiotemporal drought variability in the Mediterranean over the last 900 years. J. Geophys. Res. Atmos. 121, 2060–2074.

Cook, E., 1985. A time series analysis approach to tree ring standardization. University of Arizona, Lamont-Doherty Geol. Obs.

Cook, E.R., Briffa, K., Shiyatov, S., Mazepa, V., 1990. Tree-ring standardization and growth-trend estimation. Methods Dendrochronol. Appl. Environ. Sci. 104–123.

Donoso, C., 1982. Reseña ecológica de los bosques mediterráneos de Chile. Bosque 4, 117–146.

Donoso, P.J., Otero, L.A., 2005. Hacia una definición de país forestal:¿ Dónde se sitúa Chile? Bosque (Valdivia) 26, 5–18.

Donoso, S.R., Pena-Rojas, K., Delgado-Flores, C., Riquelme, A., Paratori, M., 2010. Above-ground biomass accumulation and growth in a marginal Nothofagus macrocarpa forest in central Chile. Interciencia 35, 65–69.

Dorado-Liñán, I., Zorita, E., Martínez-Sancho, E., Gea-Izquierdo, G., Di Filippo, A., Gutiérrez, E., Levanic, T., Piovesan, G., Vacchiano, G., Zang, C., 2017. Large-scale atmospheric circulation enhances the Mediterranean East-West tree growth contrast at rear-edge deciduous forests. Agric. For. Meteorol. 239, 86–95.

Franklin, J.F., Shugart, H.H., Harmon, M.E., 1987. Tree death as an ecological process. Bioscience 37, 550–556.

Fritts, H.C., 1976. Tree rings and climate. Elsevier.

Gajardo, R., 2001. Antecedentes sobre el "roble de Santiago" o "roble blanco"(Nothofagus macrocarpa) y sus problemas de conservación. Rev. Bosque Nativ. 28, 3–7.

Galiano, L., Martínez-Vilalta, J., Lloret, F., 2010. Drought-induced multifactor decline of Scots pine in the Pyrenees and potential vegetation change by the expansion of co-occurring oak species. Ecosystems 13, 978–991.

Garreaud, R., Alvarez-Garreton, C., Barichivich, J., Boisier, J.P., Christie, D., Galleguillos, M., LeQuesne, C., McPhee, J., Zambrano, M., 2017. The 2010-2015 mega drought in Central Chile: Impacts on regional hydroclimate and vegetation. Hydrol. Earth Syst. Sci. (in press) http://www.dgf.uchile.cl/rene/PUBS/hess-2017-191.pdf).

Garreaud, R.D., Vuille, M., Compagnucci, R., Marengo, J., 2009. Present-day South American climate. Palaeogeogr. Palaeoclimatol. Palaeoecol. 281, 180–195. http://dx.doi.org/10.1016/j.palaeo.2007.10.032.

Gazol, A., Camarero, J.J., Anderegg, W.R.L., Vicente-Serrano, S.M., 2017. Impacts of droughts on the growth resilience of Northern Hemisphere forests. Glob. Ecol. Biogeogr. 26, 166–176.

Gea-Izquierdo, G., Cañellas, I., 2014. Local climate forces instability in long-term productivity of a Mediterranean oak along climatic gradients. Ecosystems 17, 228–241.

Gea-Izquierdo, G., Viguera, B., Cabrera, M., Cañellas, I., 2014. Drought induced decline could portend widespread pine mortality at the xeric ecotone in managed mediterranean pine-oak woodlands. For. Ecol. Manage. 320, 70–82.

González-Reyes, Á., 2016. Ocurrencia de eventos de sequías en la ciudad de Santiago de Chile desde mediados del siglo XIX. Rev. Geogr. Norte Gd. 21–32.

Granda, E., Rossatto, D.R., Camarero, J.J., Voltas, J., Valladares, F., 2014. Growth and carbon isotopes of Mediterranean trees reveal contrasting responses to increased carbon dioxide and drought. Oecologia 174, 307–317.

Hernández, A., Miranda, M.D., Arellano, E.C., Dobbs, C., 2016. Landscape trajectories and their effect on fragmentation for a Mediterranean semi-arid ecosystem in Central Chile. J. Arid Environ. 127, 74–81.

Holmes, R.L., 1992. Dendrochronology program library. Lab. tree-ring Res. Univ, Arizona, Tucson.

Holmes, R.L., Adams, R.K., Fritts, H.C., Laboratory of Tree-Ring Research, U. of A., 1986. Tree-Ring Chronologies of Western North America: California, Eastern Oregon and Northern Great Basin with Procedures Used in the Chronology Development Work Including Users Manuals for Computer Programs COFECHA and ARSTAN, The Univer. ed, Laboratory of Tree-Ring Research Archives. Tucson. http://hdl.handle.net/10150/304672.

Labuhn, I., Daux, V., Girardclos, O., Stievenard, M., Pierre, M., Masson-Delmotte, V., 2016. French summer droughts since 1326 CE: a reconstruction based on tree ring cellulose δ 18 O. Clim. Past 12, 1101–1117.

Lara, A., Bahamondez, A., González-Reyes, A., Muñoz, A.A., Cuq, E., Ruiz-Gómez, C., 2015. Reconstructing streamflow variation of the Baker River from tree-rings in Northern Patagonia since 1765. J. Hydrol. 529, 511–523.

Lara, A., Villalba, R., Wolodarsky-Franke, A., Aravena, J.C., Luckman, B.H., Cuq, E., 2005. Spatial and temporal variation in Nothofagus pumilio growth at tree line along its latitudinal range (35 40′–55 S) in the Chilean Andes. J. Biogeogr. 32, 879–893.

Lavergne, A., Daux, V., Villalba, R., Barichivich, J., 2015. Temporal changes in climatic limitation of tree-growth at upper treeline forests: Contrasted responses along the west-to-east humidity gradient in Northern Patagonia. Dendrochronologia 36, 49–59.

Le Quesne, C., Acuña, C., Boninsegna, J.A., Rivera, A., Barichivich, J., 2009. Long-term glacier variations in the Central Andes of Argentina and Chile, inferred from historical records and tree-ring reconstructed precipitation. Palaeogeogr. Palaeoclimatol. Palaeoecol. 281, 334–344.

Le Quesne, C., Stahle, D.W., Cleaveland, M.K., Therrell, M.D., Aravena, J.C., Barichivich, J., 2006. Ancient Austrocedrus tree-ring chronologies used to reconstruct central Chile precipitation variability from AD 1200 to 2000. J. Clim. 19, 5731–5744.

Linares, J.C., Camarero, J.J., 2012. From pattern to process: linking intrinsic water-use efficiency to drought-induced forest decline. Glob. Chang. Biol. 18, 1000–1015.

Luebert, F., Pliscoff, P., 2006. Sinopsis bioclimática y vegetacional de Chile. Santiago.

Marshall, G.J., 2003. Trends in the southern annular mode from observations and reanalyses. J. Clim. 16, 4134–4143. http://dx.doi.org/10.1175/1520-0442(2003)016<4134:titsam>2.0.co;2.

Miranda, A., Altamirano, A., Cayuela, L., Lara, A., González, M., 2016. Native forest loss in the Chilean biodiversity hotspot: revealing the evidence. Reg. Environ. Chang. 1–13.

Montecinos, A., Aceituno, P., 2003. Seasonality of the ENSO-related rainfall variability in central Chile and associated circulation anomalies. J. Clim. 16, 281–296.

Muggeo, V.M.R., 2008. Segmented: an R package to fit regression models with broken-line relationships. R news 8, 20–25.

Mundo, I.A., El Mujtar, V.A., Perdomo, M.H., Gallo, L.A., Villalba, R., Barrera, M.D., 2010. Austrocedrus chilensis growth decline in relation to drought events in northern Patagonia, Argentina. Trees 24, 561–570.

Muñoz, A.A., González-Reyes, A., Lara, A., Sauchyn, D., Christie, D., Puchi, P., Urrutia-Jalabert, R., Toledo-Guerrero, I., Aguilera-Betti, I., Mundo, I., 2016. Streamflow variability in the Chilean Temperate-Mediterranean climate transition (35°S–42°S) during the last 400 years inferred from tree-ring records. Clim. Dyn. 1–16.

Myers, N., Mittermeier, R.A., Mittermeier, C.G., da Fonseca, G.A.B., Kent, J., 2000. Biodiversity hotspots for conservation priorities. Nature 403, 853–858. http://dx.doi.org/10.1038/35002501.

Negron, J.F., McMillin, J.D., Anhold, J.A., Coulson, D., 2009. Bark beetle-caused mortality in a drought-affected ponderosa pine landscape in Arizona, USA. For. Ecol. Manage. 257, 1353–1362.

Nehrbass-Ahles, C., Babst, F., Klesse, S., Nötzli, M., Bouriaud, O., Neukom, R., Dobbertin, M., Frank, D., 2014. The influence of sampling design on tree-ring-based quantification of forest growth. Glob. Chang. Biol. 20, 2867–2885.

Quintana, J., 2000. The drought in Chile and la Niña. Drought Netw. News 71.

Quintana, J.M., Aceituno, P., 2012. Changes in the rainfall regime along the extratropical west coast of South America (Chile): 30–43º S. Atmósfera 25, 1–22.

R core Team, R., 2017. R language definition. Vienna, Austria R Found. Stat. Comput.

Rasband, W.S., 1997. Image J, US National Institutes of Health, Bethesda, Maryland, USA, 2014.

Rigling, A., Bigler, C., Eilmann, B., Feldmeyer-Christe, E., Gimmi, U., Ginzler, C., Graf, U., Mayer, P., Vacchiano, G., Weber, P., 2013. Driving factors of a vegetation shift from Scots pine to pubescent oak in dry Alpine forests. Glob. Chang. Biol. 19, 229–240.

Rodríguez-Catón, M., Villalba, R., Morales, M., Srur, A., 2016. Influence of droughts on Nothofagus pumilio forest decline across northern Patagonia, Argentina. Ecosphere 7.

Rozas, V., Camarero, J.J., Sangüesa-Barreda, G., Souto, M., García-González, I., 2015. Summer drought and ENSO-related cloudiness distinctly drive Fagus sylvatica growth near the species rear-edge in northern Spain. Agric. For. Meteorol. 201, 153–164.

Sala, O.E., Chapin, F.S., Armesto, J.J., Berlow, E., Bloomfield, J., Dirzo, R., Huber-Sanwald, E., Huenneke, L.F., Jackson, R.B., Kinzig, A., 2000. Global biodiversity scenarios for the year 2100. Science (80-.) 287, 1770–1774.

Sarris, D., Christodoulakis, D., Körner, C., 2011. Impact of recent climatic change on growth of low elevation eastern Mediterranean forest trees. Clim. Change 106, 203–223.

Schiappacasse, I., Nahuelhual, L., Vásquez, F., Echeverría, C., 2012. Assessing the benefits and costs of dryland forest restoration in central Chile. J. Environ. Manage. 97, 38–45.

Schulman, E., 1956. Dendroclimatic changes in semiarid America. Dendroclimatic Chang. semiarid Am.

Schulz, J.J., Cayuela, L., Echeverria, C., Salas, J., Benayas, J.M.R., 2010. Monitoring land cover change of the dryland forest landscape of Central Chile (1975–2008). Appl. Geogr. 30, 436–447. http://dx.doi.org/10.1016/j.apgeog.2009.12.003.

Stokes, M.A., 1996. An introduction to tree-ring dating. University of Arizona Press.

Thompson, D.W.J., Solomon, S., Kushner, P.J., England, M.H., Grise, K.M., Karoly, D.J., 2011. Signatures of the Antarctic ozone hole in Southern Hemisphere surface climate change. Nat. Geosci. 4, 741–749.

Thompson, D.W.J., Wallace, J.M., 2000. Annular modes in the extratropical circulation. Part I: Month-to-month variability. J. Clim. 13, 1000–1016. http://dx.doi.org/10.1175/1520-0442(2000)013<1000:amitec>2.0.co;2.

Torrence, C., Compo, G.P., 1998. A practical guide to wavelet analysis. Bull. Am. Meteorol. Soc. 79, 61–78.

Trenberth, K.E., 1997. The definition of El Nino. Bull. Am. Meteorol. Soc. 78, 2771–2777. http://dx.doi.org/10.1175/1520-0477(1997)078<2771:tdoeno>2.0.co;2.

Urrutia, R.B., Lara, A., Villalba, R., Christie, D.A., Le Quesne, C., Cuq, A., 2011. Multicentury tree ring reconstruction of annual streamflow for the Maule River watershed in south central Chile. Water Resour. Res. 47, 15. http://dx.doi.org/10.1029/2010wr009562.

Vennetier, M., Vila, B., Liang, E.Y., Guibal, F., Thabeet, A., Gadbin-Henry, C., 2007. Impact of climate change on pine forest productivity and on the shift of a bioclimatic limit in a Mediterranean area. Options Méditerranéennes, Série A 75, 189–197.

Vicente-Serrano, S.M., Beguería, S., Lopez-Moreno, J.I., 2010. A multiscalar drought index sensitive to global warming: the standardized precipitation evapotranspiration index. J. Clim. 23, 1696–1718. http://dx.doi.org/10.1175/2009jcli2909.1.

Villagrán, C.M., 1995. Quaternary history of the Mediterranean vegetation of Chile. In: Ecology and Biogeography of Mediterranean Ecosystems in Chile, California, and Australia. Springer, pp. 3–20.

Villalba, R., Lara, A., Masiokas, M.H., Urrutia, R., Luckman, B.H., Marshall, G.J., Mundo, I.A., Christie, D.A., Cook, E.R., Neukom, R., Allen, K., Fenwick, P., Boninsegna, J.A., Srur, A.M., Morales, M.S., Araneo, D., Palmer, J.G., Cuq, E., Aravena, J.C., Holz, A., LeQuesne, C., 2012. Unusual Southern Hemisphere tree growth patterns induced by changes in the Southern Annular Mode. Nat. Geosci. 5, 793–798. http://dx.doi.org/10.1038/ngeo1613.

Wigley, T.M.L., Briffa, K.R., Jones, P.D., 1984. On the average value of correlated time-series, with applications in dendroclimatology and hydrometeorology. J. Clim. Appl. Meteorol. 23, 201–213. http://dx.doi.org/10.1175/1520-0450(1984)023<0201:otavoc>2.0.co;2.

Wolter, K., Timlin, M.S., 2011. El Niño/Southern Oscillation behaviour since 1871 as diagnosed in an extended multivariate ENSO index (MEI. ext). Int. J. Climatol. 31, 1074–1087.